Mutation in the TCRα subunit constant gene (*TRAC*) leads to a human immunodeficiency disorder characterized by a lack of TCRαβ+ T cells

Neil V. Morgan,[1] Sarah Goddard,[2] Tony S. Cardno,[3] David McDonald,[4] Fatimah Rahman,[1] Dawn Barge,[5] Andrew Ciupek,[3] Anna Straatman-Iwanowska,[1] Shanaz Pasha,[1] Mary Guckian,[2] Graham Anderson,[6] Aarnoud Huissoon,[2] Andrew Cant,[7] Warren P. Tate,[3] Sophie Hambleton,[4,7] and Eamonn R. Maher[1,8]

[1]Wellchild Paediatric Research Centre, Department of Medical and Molecular Genetics and Centre for Rare Diseases and Personalised Medicine, University of Birmingham School of Medicine, Birmingham, United Kingdom. [2]Regional Department of Immunology, Heartlands Hospital, Birmingham, United Kingdom. [3]Department of Biochemistry, University of Otago, Dunedin, New Zealand. [4]Institute of Cellular Medicine, Newcastle University, Newcastle upon Tyne, United Kingdom. [5]Regional Immunology Laboratory, Royal Victoria Infirmary, Newcastle upon Tyne, United Kingdom. [6]MRC Centre for Immune Regulation, The Medical School, University of Birmingham, Birmingham, United Kingdom. [7]Paediatric Immunology and Infectious Diseases Service, Great North Children's Hospital, Newcastle upon Tyne, United Kingdom. [8]West Midlands Regional Genetics Service, Birmingham Women's Hospital, Birmingham, United Kingdom.

Inherited immunodeficiency disorders can be caused by mutations in any one of a large number of genes involved in the function of immune cells. Here, we describe two families with an autosomal recessive inherited immunodeficiency disorder characterized by increased susceptibility to infection and autoimmunity. Genetic linkage studies mapped the disorder to chromosomal region 14q11.2, and a homozygous guanine-to-adenine substitution was identified at the last base of exon 3 immediately following the translational termination codon in the TCRα subunit constant gene (*TRAC*). RT-PCR analysis in the two affected individuals revealed impaired splicing of the mRNA, as exon 3 was lost from the *TRAC* transcript. The mutant TCRα chain protein was predicted to lack part of the connecting peptide domain and all of the transmembrane and cytoplasmic domains, which have a critical role in the regulation of the assembly and/or intracellular transport of TCR complexes. We found that T cells from affected individuals were profoundly impaired for surface expression of the TCRαβ complex. We believe this to be the first report of a disease-causing human *TRAC* mutation. Although the absence of TCRαβ+ T cells in the affected individuals was associated with immune dysregulation and autoimmunity, they had a surprising level of protection against infection.

Introduction

Inherited immunodeficiencies have provided novel insights into T and B cell development and immune function. Failure of T cell development, of whatever cause, produces the clinical syndrome of SCID, characterized by profound susceptibility to opportunistic infection, failure to thrive, and death in infancy. In contrast, genetic disorders that impair T cell function may display a range of phenotypes; from SCID, through partial immunodeficiency with dysregulation and/or lymphoid neoplasia, to predominant autoimmunity (1, 2).

We investigated two consanguineous families with what we believe to be a novel immune dysregulatory disorder and performed gene mapping and identification studies, which led to the identification of a mutation in the TCRα subunit constant gene (*TRAC*).

Results

Clinical features. Two apparently unrelated children from consanguineous families of Pakistani origin were noted to have clinical and immunophenotypic features in common. They presented at the ages of 15 months (family 1 [F1]; II:3) and 6 months (family 2 [F2]; II:2) with features of combined immunodeficiency: recurrent respiratory tract infection, otitis media, candidiasis, diarrhea, and failure to thrive. These infections (Table 1) responded well to conventional treatment but recurred frequently, until the institution of continuous antibacterial and antifungal prophylaxis. One child (F1;II:3) showed clear predisposition to herpes viral infection, experiencing an unusually chronic course of varicella at age 6 as well as chronic EBV and human herpesvirus 6 (HHV6) viremia. The same child showed evidence of ongoing infective damage to the respiratory tract and was treated with long-term oral antiviral therapy and intravenous immunoglobulin. In contrast, individual F2;II:2 had an uneventful episode of varicella at age 6 years and no evidence of chronic lung damage.

In addition to immunodeficiency, both children had evidence of immune dysregulation: child F1:II:3 showed hypereosinophilia, low-titer antinuclear antibodies (ANA), vitiligo, and alopecia areata, while child F2:II:2 had hypereosinophilia, eczema, autoimmune hemolytic anemia, antilymphocyte antibodies, anti-TTG antibodies, low-titer ANA, and pityriasis rubra pilaris. In contrast, humoral immunity against vaccine antigens appeared normal (Table 1). Both children developed moderate lymphadenopathy and organomegaly (hepatomegaly in the case of F1;II:3 and hepa-

Table 1
Summary of laboratory and radiological investigations in two affected children with the immunodeficiency disorder

Test type	Parameter	F2;II:2 in pedigree (aged 2 yr 8 mo)	F1;II:3 in pedigree (aged 2 yr 2 mo)	Normal range
Differential leukocyte count	Lymphocytes	5.29	1.85	2.3×10^9 to $5.4 \times 10^9/l$
	Neutrophils	0.62	1.28	1.5×10^9 to $8 \times 10^9/l$
	Eosinophils	2.5	0.08	0.04×10^9 to $0.8 \times 10^9/l$
Lymphocyte subsets (per μl)	Lymphocytes	4,710 (100%)	4,219 (100%)	
	CD3+ (T cells)	2,356 (50%)	886 (21%)	900–4,500
	CD3+CD8+ (CD8+ T cells)	911 (19%)	291 (7%)	300–1,600
	CD3+CD4+ (CD4+ T cells)	1,293 (27%)	364 (8%)	500–2,400
	CD3+TCRγδ+	80% of CD3+ cells	45% of CD3+ cells[A]	
	CD3loTCRγδ–TCRαβ–	20% of CD3+ cells	55% of CD3+ cells[B]	0
	CD3–CD56+CD16+ (NK cells)	851 (18%)	859 (20%)	100–1,000
	CD19+ (B cells)	1082 (23%)	2,366 (55%)	200–2,100
	CD19+CD27+IgM–IgD– (class-switched memory B cells)		11% of B cells at age 5 yr	
T cell proliferation assays	PHA	S.I. 16% of control	S.I. 0.6% of control	>10% of control
	Anti-CD3	S.I. 12% of control	S.I. 5% of control	
	Tetanus	S.I. 12% of control		
	PWM	S.I. 2.6% of control	S.I. 1.4% of control	
Lymphocyte	DNA analysis	Polyclonal γ and δ TCR and IgH gene rearrangements	Consistent with clonal/oligoclonal expansion of TCRγδ T cells; TCRB rearrangement appears highly abnormal	
Immunoglobulins	IgG	15.72	7.12	4.24–10.51 g/l
	IgA	1.23	1.26	0.14–1.23 g/l
	IgM	1.69	0.69	0.48–1.68 g/l
	IgE	9187	17	<44 IU/ml
Functional antibodies	Pneumococcal	399	31	15–417
	Hib	17.54	16.9	0.81–1.38
	Tetanus	0.25	14.1	0.015–1
Autoantibodies	Direct antiglobulin test	Positive	Negative	
	IgA tissue transglutaminase	108 U/ml	14.9 U/ml	0–15
	ANA	Negative	1/50	
Microbiology		Cryptosporidium (stool), coag. neg. staph. (blood)	*Staph. aureus* (ear), *Strep. pneumoniae* (ear), Pseudomonas (ear), Rotavirus (stool), *Salmonella enteritidis* (stool), varicella zoster by PCR from skin	
Radiology		Lymphadenopathy and bowel wall thickening on USS of abdomen; porta hepatis mass with hypoechoic rim and high level echoes centrally		

[A]Of which 11% naive (CD27+CD45RA+), 26% HLA-DR+ at age 5 years. [B]Of which <1% naive (CD27+CD45RA+), 42% HLA-DR+, and 38% CD25+CD4+ at age 5 years. coag. neg. staph., coagulase-negative staphylococcus; Hib, *Haemophilus influenzae* type B; S.I., stimulation index; *Staph.*, *Staphylococcus*; *Strep.*, *Streptococcus*; USS, ultrasound scan.

tosplenomegaly in F2;II:2). At age 2 years, weight gain faltered in individual F2;II:2, and imaging revealed thickened bowel loops and a mass at the porta hepatis. Histology of the liver showed patchy eosinophilia, with biliary fibrosis and no evidence of parasites or fungi. It was felt that this may have been an autoimmune process, but infection such as cryptosporidium could not be excluded (feces were negative for cryptosporidium at this time). This child received a successful matched sibling bone marrow transplant age 7, while individual F1;II:3 underwent transplantation at age 6 years, also from a matched sibling (both children received reduced-intensity pretransplant conditioning with alemtuzumab, fludarabine, and melphalan).

Flow cytometry of peripheral blood lymphocytes. The flow cytometric peripheral blood lymphocyte profiles of the two affected individuals were strikingly similar and unusual. Conventional CD3+ T cells were present but uniformly expressed TCRγδ, with or without CD8 (Table 1, Figure 1, and data not shown). Furthermore, an abnormal population of CD3lo cells was present, which expressed TCRαβ at extremely low levels. These CD3lo cells could be further subdivided on the basis of CD4 and CD8 expression; the majority were

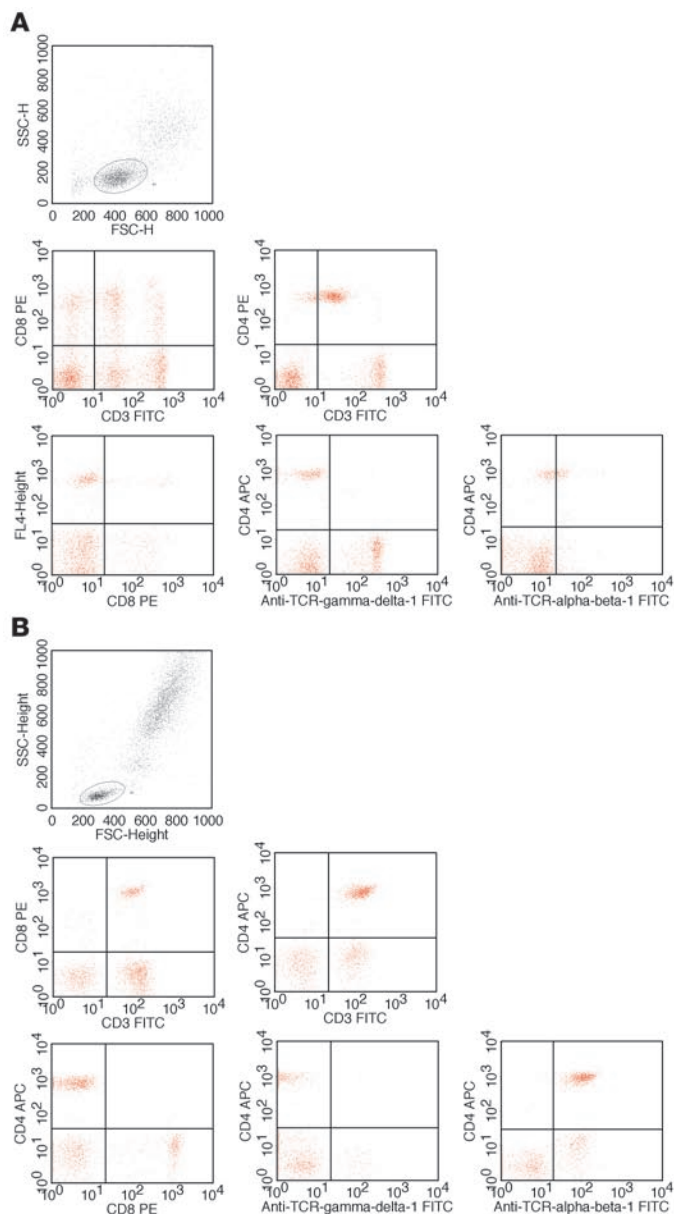**Figure 1**
Flow cytometry of peripheral blood lymphocytes. Assays were performed in whole blood using the TruCOUNT method. TCRαβ antibody WT31 from BD Biosciences — Pharmingen was used. (**A**) Child F2:II:2 at age 2 years and (**B**) 6 months after bone marrow transplantation.

Molecular genetic analysis. In light of negative results of immunological and molecular investigations for known immunodeficiency disorders, we hypothesized that both children might have a novel autosomal recessive disorder and undertook genetic linkage studies using polymorphic microsatellite markers and genome-wide SNP genotyping using the Affymetrix 250K SNP microarray (Figure 2A). Linkage to the *TRBC1* gene was excluded, and in both affected children the largest overlapping homozygous regions (1.46 Mb and 2.60 Mb) were at 14q11.2 (Figure 2A). The two children shared a common haplotype of 161 SNPs between rs7159964 (21,443,181 bp) and rs3759611 (22,906,052 bp) on chromosome 14. Genotyping of parents and siblings with microsatellite markers (D14S742, D14S283, D14S1280, and D14S275) confirmed linkage (Figure 2B). Mutation analysis of *TRAC* (chromosome 14:22,086,287–22,089,447 bp) was undertaken, revealing a homozygous G-to-A substitution (c.*1G>A) at the last nucleotide of exon 3 (immediately following the translation termination codon) in both affected children (Figure 3A). Family studies confirmed that the sequence change segregated with disease status, and the c.*1G>A mutation was not detected in 384 ethnically matched control chromosomes.

In considering possible disease mechanisms, we first investigated whether the *TRAC* c.*1G>A substitution might promote a significant increase in readthrough of the termination codon, as previously shown for certain mammalian mRNAs (particularly at genetic recoding sites; refs. 3, 4). Thus, we compared the termination efficiency of the wild-type and mutant sequences (embedded in a typical +6 to +9 context sequence) by placing each between two luciferase reporter genes (*RLuc* and *Luc+*) and assaying the relative activities of the two luciferases in human cultured cells. Although the mutant *A allele was associated with a significant increase in readthrough of the stop signal (compared with the wild-type *G), the absolute amount of readthrough product was relatively small, suggesting that this was unlikely to be the mechanism of disease in vivo (data not shown).

We next hypothesized that the c.*1G>A mutation would impair splicing of the *TRAC* transcript, since the mutation is within the consensus 5′ splice site. RT-PCR analysis of *TRAC* cDNA in members of the two affected families revealed exon skipping of the last coding exon (exon 3), resulting in an aberrant transcript joining exon 2 to the normally untranslated exon 4 (Figure 3, B and C) (testing for additional alternative patterns of *TRAC* splicing using primers anchored in exon 1 and intron 3 did not detect further transcripts). In the predicted translation product, the 35 C-terminal amino acids are replaced by 56 amino acids encoded by exon 4 (p.Thr107LeufsX56). This results in partial loss of the connecting peptide domain and abolition of the transmembrane and cytoplasmic domains of the TCRα chain. Previously, deletion of as few as 9 amino acids from the C-terminus of the TCRα chain has been reported to impair assembly and/or intracellular transport of TCR-CD3 complexes (5, 6). Additionally a conserved motif (FETDxNLN), present in the α chain connecting peptide domain, was shown to be critical in controlling antigen responsiveness (7). Therefore, the c.*1G>A mutation–associated splicing defect would be expected to have a profound impact on TCRα chain structure and function.

Cellular localization and immunoblotting of TRAC mutant. When assessed by flow cytometry, surface staining for TCRαβ was strongly reduced in patient cells (Figure 1). To assess whether TCR poly-

CD4+CD8−, while a smaller double-positive population decreased with age. Thymic emigrant equivalents (CD45RA+CD27+) were present within the CD3hi (TCRγδ+, 11%) but barely within the CD3lo (TCRγδ−, <1%) compartment. Proliferation of lymphocytes in response to phytohemagglutinin (PHA) and OKT3 was variably reduced compared with that in controls (Table 1). Despite these profound T cell abnormalities, class-switched memory B cells were present, immunoglobulin levels were within the normal range (apart from elevated IgE levels in F2;II:2), and vaccine responses were demonstrable. In keeping with these findings, the lymph node biopsy of individual F2;II:2 showed lymph node follicles and development of germinal centers (data not shown).
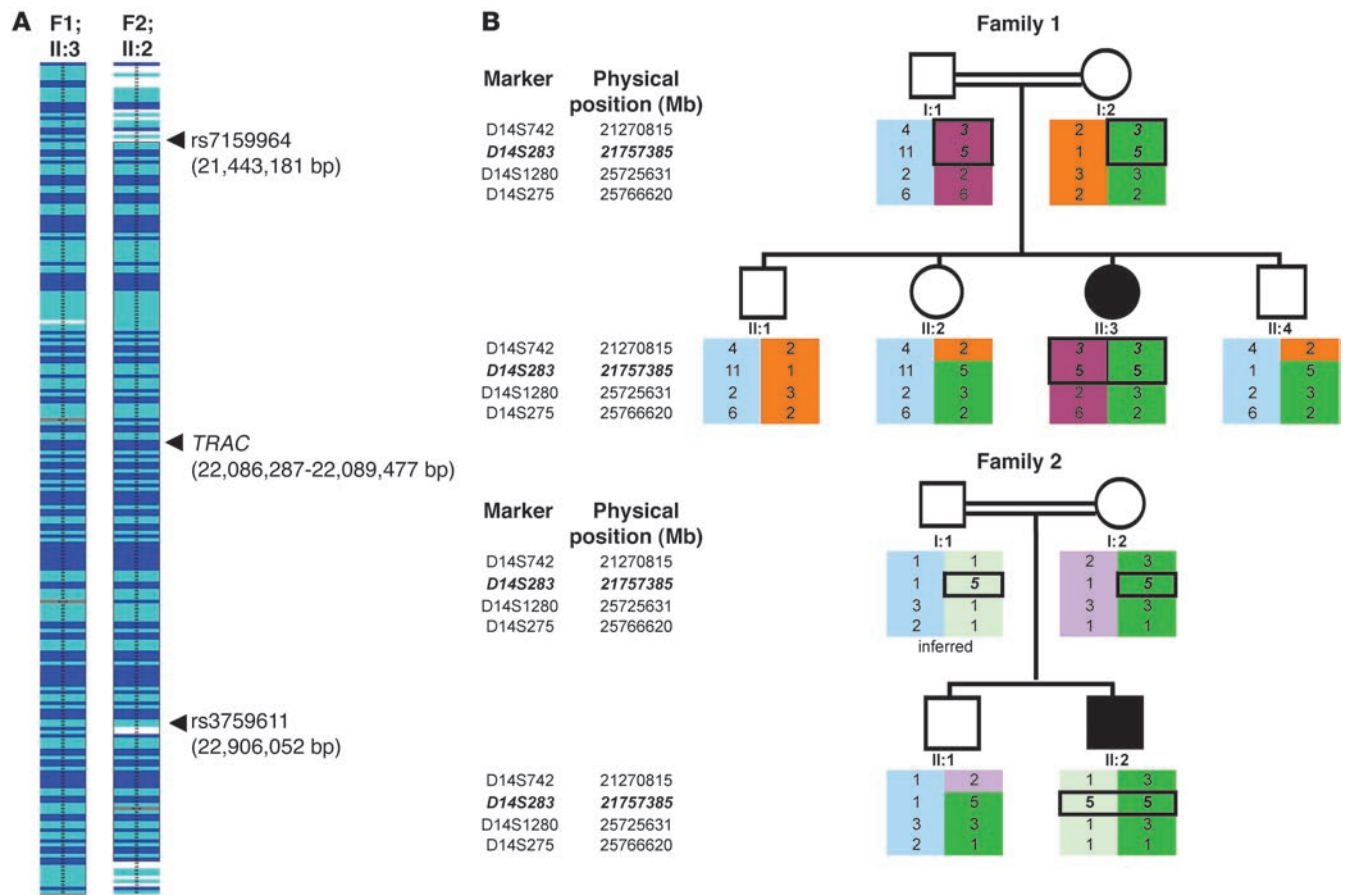
Figure 2
Candidate region of linkage at chromosome 14q11.2. (**A**) Affymetrix 250K SNP arrays in affected individuals with the immunodeficiency disorder (F1;II:3, F2;II:2) identified a common region of autozygosity (between SNPs rs7159964 [21,443,181 bp] and rs3759611 [22,906,052 bp]). Homozygous AA and BB SNPs are shown in dark blue and light blue, respectively; heterozygous AB SNPs are shown in white; and homozygous regions are boxed. (**B**) Family pedigrees and haplotypes for microsatellite markers from chromosome 14q in two families. Boxed regions indicate homozygous disease alleles. The minimal candidate interval that encompasses the disease locus is the region between markers D14S742 and D14S1280.

peptides were being retained within the cell, we prepared lysates of patient PBMCs and performed immunoblotting using antibodies against TCRα and TCRβ (Figure 4), normalizing for the proportion of TCRγδ⁻ T cells. In contrast to normal control cells, patient cells showed undetectably low expression of either TCRα or TCRβ polypeptides, suggesting that the *TRAC* mutation not only resulted in TCRα deficiency but also reduced TCRβ expression.

To investigate with greater sensitivity any effect on expression and subcellular localization of the TCRαβ complex, we immunostained patient and control PBMCs with antibodies against T cell receptor α and β chains and observed localization using immunofluorescence microscopy. In control cells, colocalization of α and β chains within distinct areas of the cell membrane was readily apparent. Patient cells showed reduced levels of expression and no evidence of colocalization (Figure 5), suggesting that the mutant α chain fails to complex normally with the TCR β chain. Consistent with this and in contrast to wild-type TCRα, mutant HA-tagged TCRα, and GFP-tagged TCRβ failed to colocalize intracellularly in transfected HeLa cells (Figure 6). Surface expression in this system could not be assessed, owing to the lack of CD3 expression.

Discussion

As well as displaying what we believe to be a novel immune disorder, the two families harbor a most unusual mutation. To our knowledge, there are no previous reports of a mutation at the base following a termination codon (c.*1) in human disease. Prokaryotes and eukaryotes demonstrate highly significant deviations from the expected nucleotide distribution before and after the stop codon (3), and the mammalian termination signal decoding factor eRF1 absolutely requires a tetranucleotide as a minimum recognition element in vitro (8). Hence, nucleotide substitutions at the base following the termination codon might cause disease by impairing the efficiency of the "tetranucleotide stop signal" (3). However, when we modeled the effect in cultured cells, we found that although the c.*1G>A mutation did cause a small increase in readthrough, this was unlikely to be sufficient to cause a clinical phenotype, and the pathogenicity of the c.*1G>A mutation was due to abnormal splicing. Hence, the apparently unique nature of the c.*1 mutation in *TRAC* appears to be due to the unusual exon/intron structure of the gene. It is not known whether c.*1 mutations in other genes might cause human disease by causing a "leaky termination signal" alone, but such an effect may only be
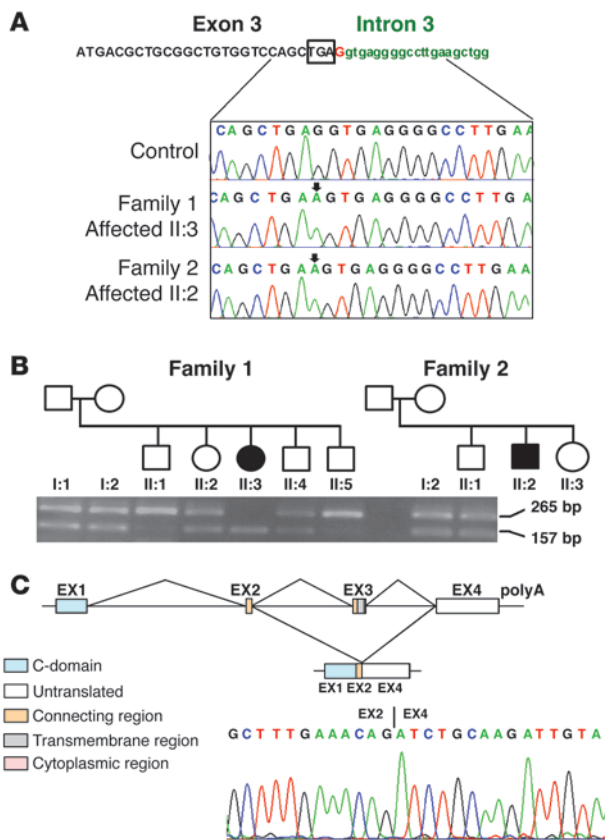
Figure 3
Identification of a homozygous G-to-A substitution in the first base following the termination codon (*1) in *TRAC*. (**A**) Wild-type and mutant *TRAC* sequence traces. The position of the *1G>A sequence change in the patients is indicated by the arrows. The boxed sequence shows the tetranucleotide translation termination signal. (**B**) RT-PCR analysis of *TRAC* showing skipping of exon 3, which segregates within the two families. (**C**) Schematic showing exon structure and domains of mutant and natively spliced mRNA and sequence trace from RT-PCR of *TRAC*, resulting in skipping of exon 3 (exon structure adapted from IMGT repertoire; http://www.imgt.org/textes/IMGTrepertoire/).

produce class-switched antibodies and germinal centers and to mount antibody responses against both vaccine and auto-antigens. In this regard, they resemble the TCRα-knockout mouse model, in which γδT cells have been proposed to provide T cell help to B cells, including those responsible for autoantibody production (11, 12). *Tcra*−/− mice possess normal numbers of double-positive and double-negative thymocytes (13), but generate few single-positive thymocytes, and most peripheral T cells bear TCRγδ. With increasing age, the mice develop an aberrant population of peripheral T lymphocytes, but these are CD3+CD4+ TCRβ+/TCRα− cells that may express TCRβ homodimers (14) or pre-TCR (15). Their appearance is temporally and possibly causally associated with the development of inflammatory bowel disease (16, 17). Thus, in the *Tcra*−/− mouse as in our human patients, the inability of single-positive thymocytes to express a mature αβTCR does not appear to prevent thymic egress absolutely but results in the development of T cells with an abnormal TCR phenotype. It would have been of great interest to clarify what signals sustained the CD3lo population within our patients, since low-level signaling via the TCR has been proposed to be essential to T cell survival. Analysis of TCR gene rearrangement within sorted CD3lo cells might also have shed light on their developmental origins. As to their functional significance, we can unfortunately say little save to observe that other partial T cell deficiencies lead to a similar combination of reduced T cell effector function and T cell dysregulation (2).
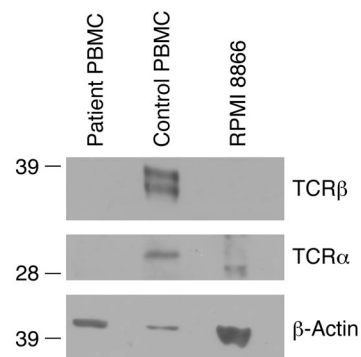
evident if the cells are sensitive to small changes in expression of the normal gene product or if the abnormal "readthrough protein" has a dominant effect on the function of the wild-type protein.

Most T cells express a heterodimeric T cell receptor consisting of β and α peptides in association with subunits of the CD3 complex (γ, δ, ε, ζ, and η chains). The antigen-binding region of the T cell receptor (the variable region) is assembled from an extensive repertoire of coding segments present in the TCR loci. During T cell development in the thymus, gene segments are rearranged to form a unique V exon in each thymocyte (9). The β chain gene is rearranged before *TRAC*, and, if productive, the TCRβ chain is initially expressed with preTα, an invariant chain. Functional signaling through this complex must occur for progression to α chain rearrangement to take place (this is known as β selection). This coincides with progression from the intermediate single-positive stage (CD3lo, CD4+, CD8−, in humans) to the double-positive stage (CD4+, CD8+). The αβ-expressing thymocyte then undergoes both positive selection (to ensure restriction to self-MHC) and negative selection to prevent recognition of self, called central tolerance (10). Defective expression of TCRα would be expected to impair αβT cell development beyond β selection because of a failure to deliver positively selecting signals. Conversely, the development of γδT cells should not be directly affected, since *TRAC* rearrangement and TCRγδ expression are mutually exclusive outcomes.

Despite lacking a critical molecule for T cell function, the two children with a homozygous *TRAC* mutation did not succumb to infection and remained relatively healthy for some years on regular antibiotic prophylaxis. Furthermore, they were able to

Figure 4
Immunoblotting of TCRα and TCRβ in patients cells, normal control cells, and negative control cells (RPMI 8866). The patient lane was overloaded to compensate for the lower number of non-γδ T cells in the patient (by densitometry, the patient sample had approximately 3 times as much actin as the control and the patient's non-γδ T cells comprised approximately 20% of total lymphocytes at the time of analysis (expected proportion in adult control is 60%–70%).
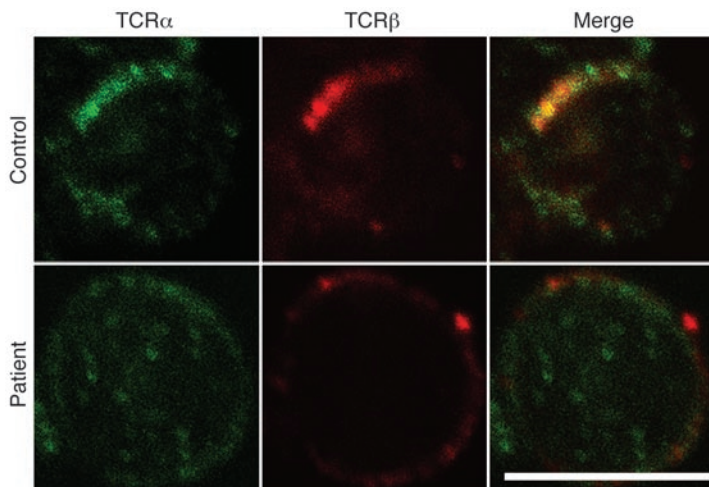
Figure 5
TRAC mutation results in mislocalization of the TCRα and -β chains. Patient and control PBMCs were incubated with antibodies against T cell receptor α and β chains and viewed by confocal microscopy. Scale bar: 6 μm.

Although the children have shown susceptibility to infection, neither opportunistic infections nor mycobacterial disease have been a feature. Cryptosporidium and salmonella have, however, been cultured during admissions to hospital with fever. Susceptibility to these pathogens is associated with defects of the IFN-γ–IL-12/23 signaling pathway as well as T cell immunodeficiencies including HLA class II deficiency (18). Infection by intracellular pathogens is also seen in the TRAC-deficient mouse model, with susceptibility to cryptosporidium, mycobacterium, and *Leishmania* (19–21). There is no evidence in the mouse model of increased risk of malignancy, although lymphadenopathy is a feature shared with our patients (22).

Finally we note that this is the second report of genetic involvement of the T cell receptor alpha locus (TRA@) in human disease, as polymorphic SNPs in TRA@ were recently found to be associated with narcolepsy (the strongest association was with an SNP close to the junctional [J] segment gene [*TRAJ10*]) (23). The absence of this sleep disorder in children with *TRAC* mutations is consistent with the suggestion that the association between narcolepsy and TRA@ may be related to an autoimmune process involving destruction of hypocretin-producing neurons (24).

Methods

Patient ascertainment and sampling. This study was conducted according to the principles expressed in the Declaration of Helsinki. The study was approved by the South Birmingham Research Ethics Committee, United Kingdom. All participants provided informed consent for the collection of samples and subsequent analysis. DNA was extracted from whole blood and extracted (Gentra, Puregene DNA purification system) for all family members.

Gene mapping. A genome-wide linkage scan was carried out using the Affymetrix 250K SNP chip in the affected individual from each family with the immunodeficiency disorder (F1;II:3 and F2;II:2). This scan identified a single region of homozygosity at chromosome 14q11.2 shared by the two affected individuals (Figure 2A). These homozygous regions were further analyzed by typing microsatellite markers (D14S742, D14S283, D14S1280, and D14S275) in all family members from whom DNA was available (Figure 2B).

Mutation analysis. We identified positional candidate genes using data from the National Center for Biotechnology Information (NCBI) and University of California Santa Cruz human genome databases. Sequenc-

ing was performed using standard methods on an ABI 3730 automated sequencer. For *TRAC*, we designed primer pairs using exon-primer (http://ihg.helmholtzmuenchen.de/ihg/EasyExonPrimer.html) to amplify coding exons 1–3. The full coding region of human *TRAC* was PCR amplified from genomic DNA with the following primers: *TRAC* exon 1 (TRAC_Exon1_FOR) 5′-CAAAGAGGGAAATGAGATCATG-3′ and (TRAC_Exon1_REV) 5′-GGCCATTCCTGAAGCAAG-3′; *TRAC* exon 2 (TRAC_Exon2_FOR) 5′-TGCCCAAGAACTAGGAGGTC-3′ and (TRAC_Exon2_REV) 5′-GGTTATTGCGGGGTTCATCAC-3′; *TRAC* exon 3 (TRAC_Exon3_FOR) 5′-GCTCTGCCTTGGGGAAAAC-3′ and (TRAC_Exon3_REV) 5′-CTGCAGGGAGGTTTGCTCTC-3′. Genomic DNA from 192 ethnically matched controls was used to screen for the identified *TRAC* mutation.

RT-PCR. Total RNA was extracted from human lymphocytes using the RNeasy Mini Kit (QIAGEN). cDNA was synthesized using random primers and AMV reverse transcriptase using the Promega reverse transcription system according to the manufacturer's instructions (A3500, Promega). RT-PCR of *TRAC* was performed using the following primers: TRAC2F (5′-GTTCCTGTGATGTCAAGCTGGTC-3′) and TRACx4R2 (5′-GGTAGCAGCTTTCACCTCCTTG-3′).

Plasmid constructs. Wild-type constructs of the full coding region of human *TRAC* and *TRBC1* were PCR amplified from cDNA with the following primers: *TRAC* (TRAC_HA_FOR) 5′-GCTAGTCGACTATATCCAGAACCCTGACCC-3′ and (TRAC_WT_REV) 5′-CGATGGTACCTCAGCTGGACCACAGCCGCA-3′; *TRBC1* (TRBC1_GFP_FOR) 5′-GCTAGTCGACTTAGGACCTGAACAAGGTGTT-3′ and (TRBC1_WT_REV) 5′-CGATGGTACCACAGAAATCCTTTCTCTTGAC-3′. The mutant *TRAC* construct was PCR amplified from cDNA with the primers (TRAC_HA_FOR) 5′-GCTAGTCGACTATATCCAGAACCCTGACCC-3′ and (TRAC_MUT_REV) 5′-CGATGGTACCCTGTTTCAAAGCTTTTCTC-3′. Forward primers contained a *Sal*I restriction site, and reverse primers contained a *Kpn*I site to allow subcloning of the PCR fragments into the pEGFP-C2 and pCMV-HA vectors (BD Biosciences — Clontech). All plasmid constructs were verified by sequencing.

Cell culture. HeLa cells were routinely maintained in DMEM (Sigma-Aldrich) supplemented with 10% fetal bovine serum at 37°C, 5% CO₂.

Cellular localization. PBMCs were obtained from patient F1;II:3 and control blood and stored frozen at –140°C in 10% DMSO, 90% fetal calf serum. After rapid thawing, cells were washed with PBS, fixed with 4% paraformaldehyde, and permeabilized with 0.1% Triton/PBS. Cells were blocked with 1% BSA and incubated with antibodies against TCRα (sc-9100) and TCRβ (sc-5277) (Santa Cruz Biotechnology Inc.). Cells were
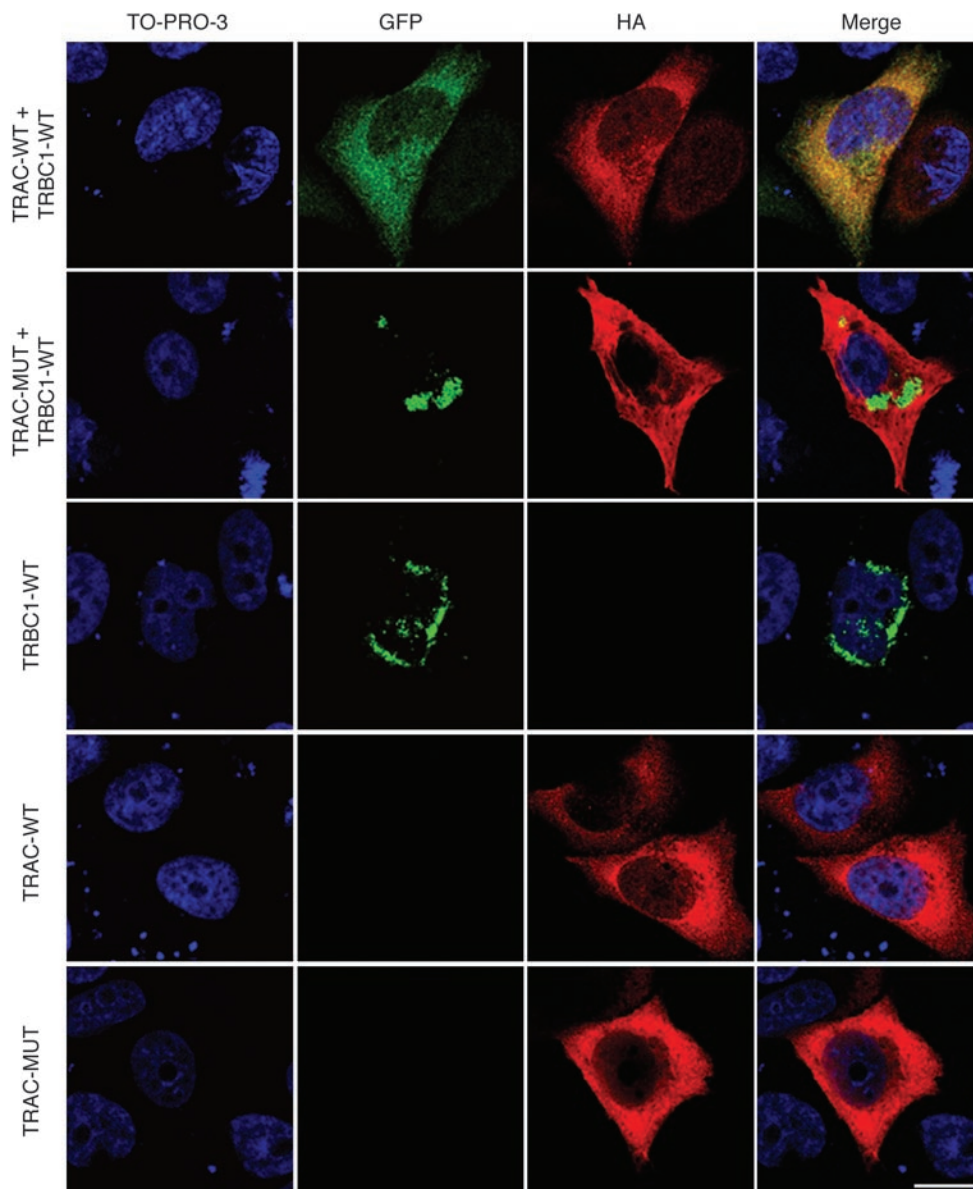
Figure 6
Cellular localization of TCRαβ complex in HeLa cells. HeLa cells grown on coverslips were cotransfected with pCMV.HA-*TRAC* and pEGFP-*TRBC1* (top row), pCMV.HA-*TRAC*exon1–2 and pEGFP-*TRBC1* (second row), pEGFP-*TRBC1* (third row), pCMV.HA-*TRAC* (fourth row), and pCMV.HA-*TRAC*exon1–2 (fifth row). Cells were labeled with anti-HA antibody, followed by Alexa Fluor 546–conjugated secondary antibody, and nuclei were stained with TO-PRO-3 iodide. Cells were visualized with a confocal microscope. Scale bar: 15 μm.

washed and incubated with anti-rabbit Alexa Fluor 488 and anti-mouse Alexa Fluor 546 conjugates (Invitrogen). After washing, cells were mounted using ProLong Gold antifade and examined by confocal microscopy using a Leica SP2 confocal microscope.

HeLa cells were grown on coverslips in 24-well plates and transfected with 1 μg of plasmid DNA constructs (pCMV-HA, pCMV-HA.TRAC.WT, pCMV-HA.TRAC.MUT, pEGFP vector, and pEGFP.TRBC1.WT) using Lipofectamine 2000 (Invitrogen) according to the manufacturer's instructions. After 24 hours, cells were washed with PBS, fixed in 4% paraformaldehyde, and permeabilized. The subcellular distribution of HA.TRAC was assessed by incubating cells with mouse monoclonal antibodies against HA (Sigma-Aldrich), detected using Alexa Fluor 546 conjugate (Invitrogen), and

nuclei were stained using TO-PRO-3 iodide (Invitrogen). Finally, cells were mounted using Citifluor (Citifluor Ltd.), and images were visualized using a Leica SP2 confocal microscope.

Immunoblotting. Control and patient PBMCs and RPMI 8866 cells were lysed for 10 minutes on ice in lysis buffer (20 mM Tris-HCl, pH 7.4; 150 mM sodium chloride; 1% Triton-X 100; 5 mM EDTA; Halt protease inhibitors [Pierce]) before clarification at 13,000 *g*. Lysates were reduced (5 minutes at 70°C, LDS sample buffer and reducing agent [Invitrogen]) and alkylated (10 minutes at room temperature, 50 mM iodoacetamide) and electrophoresed at 25 mA/gel on duplicate 10% SDS polyacrylamide gels. Proteins were transferred to PVDF membrane at 30 mA/gel for 120 minutes. After blocking for 1 hour in 5% milk in TBS-0.5% Tween-20 (TBST), membranes were cut and

probed with 0.4 µg/ml anti-TCRα (H-142, Santa Cruz Biotechnology Inc.), anti-TCRβ (G-11, Santa Cruz Biotechnology Inc.), or anti–β-actin (AC-74, Sigma-Aldrich) overnight at 4°C in 5% milk in TBST. After 4 washings of 5 minutes each in TBST, blots were incubated with the appropriate secondary antibody (10–20 ng/ml goat anti–mouse HRP or 20 ng/ml goat anti–rabbit HRP) for 1 hour. Blots were washed a further 4 times prior to incubation with chemiluminescent substrate (West Dura, Pierce) and exposure to film.

Address correspondence to: Eamonn R. Maher, Department of Medical and Molecular Genetics, University of Birmingham, Institute of Biomedical Research, Edgbaston, Birmingham, B15 2TT, United Kingdom. Phone: 44.121.627.2741; Fax: 44.121.414.2538; E-mail: e.r.maher@bham.ac.uk.

1. Fischer A. Human primary immunodeficiency diseases. *Immunity*. 2007;27(6):835–845.
2. Liston A, Enders A, Siggs OM. Unravelling the association of partial T-cell immunodeficiency and immune dysregulation. *Nat Rev Immunol*. 2008;8(7):545–558.
3. McCaughan KK, Brown CM, Dalphin ME, Berry MJ, Tate WP. Translational termination efficiency in mammals is influenced by the base following the stop codon. *Proc Natl Acad Sci U S A*. 1995; 92(12):5431–5435.
4. Cridge AG, Major LL, Mahagaonkar AA, Poole ES, Isaksson LA, Tate WP. Comparison of characteristics and function of translation termination signals between and within prokaryotic and eukaryotic organisms. *Nucleic Acids Res*. 2006; 34(7):1959–1973.
5. Shelton JG, Gülland S, Nicolson K, Kearse KP, Bäckström BT. Importance of the T cell receptor alpha-chain transmembrane distal region for assembly with cognate subunits. *Mol Immunol*. 2001; 38(4):259–265.
6. Bhatnagar A, et al. Mutational analysis of conserved amino acids in the T cell receptor alpha-chain transmembrane region: a critical role of leucine 112 and phenylalanine 127 for assembly and surface expression. *Mol Immunol*. 2003;39(15):953–963.
7. Bäckström BT, Milia E, Peter A, Jaureguiberry B, Baldari CT, Palmer E. A motif within the T cell receptor α chain constant region connecting peptide domain controls antigen responsiveness. *Immunity*. 1996;5(5):437–447.

8. Poole ES, Major LL, Mannering SA, Tate WP. Translational termination in *Escherichia coli*: three bases following the stop codon crosslink to release factor 2 and affect the decoding efficiency of UGA - containing signals. *Nucleic Acids Res*. 1998;26(4):954–960.
9. Davis MM, Bjorkman PJ. T-cell antigen receptor genes and T-cell recognition. *Nature*. 1988; 334(6181):395–402.
10. Anderson G, Moore NC, Owen JJ, Jenkinson EJ. Cellular interactions in thymocyte development. *Annu Rev Immunol*. 1996;14:73–99.
11. Mombaerts P, et al. Mutations in T-cell antigen receptor genes alpha and beta block thymocyte development at different stages. *Nature*. 1992; 360(6401):225–231.
12. Wen L, et al. Immunoglobulin synthesis and generalized autoimmunity in mice congenitally deficient in alpha beta(+) T cells. *Nature*. 1994; 369(6482):654–658.
13. Eichelberger M, McMickle A, Blackman M, Mombaerts P, Tonegawa S, Doherty PC. Functional analysis of the TCR alpha- beta+ cells that accumulate in the pneumonic lung of influenza virus-infected TCR-alpha−/− mice. *J Immunol*. 1995;154(4):1569–1576.
14. Takahashi I, Iijima H, Katashima R, Itakura M, Kiyono H. Clonal expansion of CD4+ TCRbetabeta+ T cells in TCR alpha-chain- deficient mice by gut-derived antigens. *J Immunol*. 1999;162(3):1843–1850.
15. Barber DF, Passoni L, Wen L, Geng L, Hayday AC. The expression in vivo of a second isoform of pT alpha: implications for the mechanism of pT alpha action. *J Immunol*. 1998;161(1):11–16.

16. Wen L, et al. Germinal center formation, immunoglobulin class switching, and autoantibody production driven by "non alpha/beta" T cells. *J Exp Med*. 1996;183(5):2271–2282.
17. Takahashi I, Kiyono H, Hamada S. CD4+ T-cell population mediates development of inflammatory bowel disease in T-cell receptor alpha chain-deficient mice. *Gastroenterology*. 1997;112(6):1876–1886.
18. Casanova JL, Abel L. The human model: a genetic dissection of immunity to infection in natural conditions. *Nat Rev Immunol*. 2004;4(1):55–66.
19. Waters WR, Harp JA. Cryptosporidium parvum infection in T-cell receptor (TCR)-alpha- and TCR-delta-deficient mice. *Infect Immun*. 1996; 64(5):1854–1857.
20. Mogues T, Goodrich ME, Ryan L, LaCourse R, North RJ. The relative importance of T cell subsets in immunity and immunopathology of airborne Mycobacterium tuberculosis infection in mice. *J Exp Med*. 2001;193(3):271–280.
21. Satoskar A, Okano M, David JR. Gamma delta T cells are not essential for control of cutaneous Leishmania major infection in genetically resistant C57BL/6 mice. *J Infect Dis*. 1997;176(6):1649–1652.
22. Viney JL, et al. Lymphocyte proliferation in mice congenitally deficient in T-cell receptor alpha beta + cells. *Proc Natl Acad Sci U S A*. 1994;91(25):11948–11952.
23. Hallmayer J, et al. Narcolepsy is strongly associated with the T-cell receptor alpha locus. *Nat Genet*. 2009;41(6):708–711.
24. Vyse TJ. Narcolepsy and the T-cell receptor. *Nat Genet*. 2009;41(6):640–641.